

Role of Cavitation in Bulk Ultrasound Ablation: A Histologic Study

Chandra Priya Karunakaran, Mark T. Burgess, Christy K. Holland,
and T. Douglas Mast

Department of Biomedical Engineering, University of Cincinnati, Cincinnati, Ohio

Abstract. The role of cavitation in bulk ultrasound ablation has been evaluated in a series of *in vitro* experiments. Fresh bovine liver tissue was ablated with a 3.1 MHz ultrasound image-ablate probe at 31 W/cm² for 20 minutes under normal and elevated ambient pressures. A 1 MHz passive cavitation detector recorded acoustic emission signals which were quantified by computation of average subharmonic, broadband, and low-frequency emission levels. After ablation, tissue was sliced and stained with 2% TTC to evaluate thermal damage. Emission levels were quantified and correlated with tissue ablation histology. The results indicate that bubble activity significantly affects heat deposition in ultrasound bulk ablation, in a manner different from high-intensity focused ultrasound (HIFU) ablation.

Keywords: Bulk ultrasound ablation, passive cavitation detection, TTC staining.

PACS: 43.80.Sh, 43.35.Ei, 43.80.Gx

INTRODUCTION

Liver and intrahepatic bile duct cancer is a major public health problem, with 21,370 new cases and 18,410 deaths estimated to occur during 2008 (National Cancer Institute, 2008). Ultrasound ablation techniques have potential advantages for liver cancer treatment compared to radiofrequency and microwave ablation, including reduced invasiveness and greater treatment selectivity (Fry 1993). The therapy modality considered here is bulk ultrasound ablation, in which tissue is exposed to unfocused or weakly-focused ultrasound at acoustic intensities lower than HIFU (<100 W/cm²), resulting in thermal ablation at volumetric rates of ~1 ml/min or higher (Mast 2005, 2008).

Therapeutic ultrasound is known to produce acoustic cavitation, defined as the formation and destruction of microbubbles due to alternating compressional and rarefactional pulses of ultrasound (ter Haar 1981, Rabkin 2001). Effects of cavitation in therapeutic ultrasound include tissue fragmentation (Xu 2005), enhancement of thermal lesion depth (Melodelima 2003), and alteration of thermal lesion geometry (Fry 1993, Watkin 1996, Bailey 2001, Reed 2003). Suppression of cavitation during HIFU ablation, achieved by use of overpressure, has been shown to reduce “tadpole” shaped distortions of thermal lesions (Bailey 2001) and to increase HIFU lesion size (Reed 2003).

Here, the role of cavitation in ultrasound bulk ablation was studied in a series of *in vitro* ablation experiments, performed at elevated pressure to suppress bubble activity and at normal pressure. Similar to a previous study (Mast 2008), passive cavitation

detection was performed throughout ablation exposures to quantify subharmonic, broadband, and low-frequency emissions caused by acoustic cavitation and vaporization. Tissue damage was quantified by TTC vital staining and then correlated with measured acoustic emission levels. The results indicate significant differences in acoustic emission and ablation results between the two pressure levels.

MATERIALS AND METHODS

The constructed pressure chamber and experimental setup is shown in Figure 1. A pressure chamber was constructed using a polyethylene terephthalate (PET) bottle (9.3 length, 3.3 cm diameter, 0.8 mm wall thickness) which was threaded onto a galvanized iron pipe reducer, and in turn connected to a hydraulic hand pump (Ralston Instruments). Bovine liver tissue was obtained from a local slaughterhouse, immediately placed in 0°C phosphate buffered saline (PBS), and used within 12 hours *post mortem*. Immediately before each exposure, tissue blocks were cut to 8.5×3.5×3 cm³ and placed in the pressure chamber, which was then filled with degassed PBS. The pressure chamber was placed in a glass tank filled with degassed, deionized water and its surface was cleaned with a soft brush to remove any adhering bubbles.

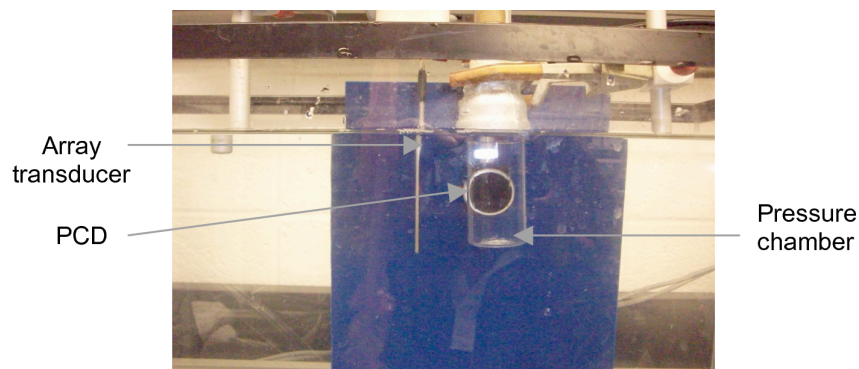


FIGURE 1. Photograph of experimental setup showing the transparent pressure chamber, 3.1 MHz image-ablate ultrasound array, and 1 MHz PCD.

The setup for ablation experiments, similar to a previous study (Mast 2008) except for the pressure chamber, employed sonication by a 3 mm diameter, 32 element, 3.1 MHz image-ablate ultrasound array (Makin 2005; THX 3N, Guided Therapy Systems). Passive cavitation detection (PCD) was performed by a 1 MHz, 25 mm circular unfocused receiver (C302, Panametrics). The image-ablate array was placed at a distance of 8 mm from the bottle surface (13-15 mm from tissue surface) with the active surface facing the liver capsule. The PCD was placed perpendicular to the direction of sound propagation, 10-15 mm from the bottle surface. The chamber was then pressurized to 175 psi (1.1 MPa) through the PBS-filled hand pump for 11 overpressure experiments, and was not pressurized for 11 control experiments.

Ultrasound exposures were programmed and controlled using the Iris imaging and ablation system (Makin 2005; Guided Therapy Systems). For all exposures, the 16 center array elements, comprising an unfocused 2.3×24.5 mm² active aperture, were

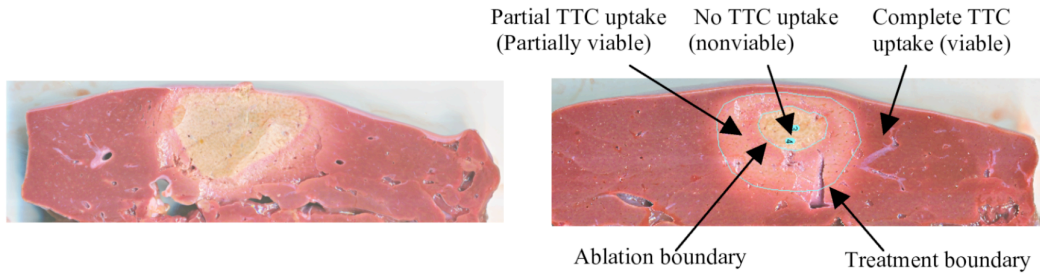


FIGURE 2. Representative TTC-stained cross sections of bovine liver tissue after ultrasound bulk ablation. Left: control (normal pressure) conditions. Right: overpressure conditions, with annotations showing segmentation of ablated and treated regions based on TTC uptake.

fired at 3.1 MHz to produce a beam of 30 W/cm^2 estimated *in situ* intensity (1.0 MPa pressure amplitude) for 20 minutes. PCD signals of length 1 s were amplified by a low-noise preamplifier (SR 560, Stanford Research Systems) with an amplitude gain of 200, and recorded by a digital oscilloscope (Lecroy Waverunner 6050A) with a sampling rate of 1 MHz at 2.6 s intervals. Power spectra for each PCD signal were estimated by the periodogram method using 1000-point FFTs with rectangular windowing and 1000 averages over the 1 s signal duration.

For each treatment, acoustic emission levels were quantified as the total spectral energy within three distinct frequency bands: subharmonic (1.55 MHz), broadband (0.3-0.75 MHz), and low-frequency (10-30 kHz). Average emission levels were determined by computing the average dB-scaled power spectrum level, relative to the measured frequency-dependent noise floor, for each 20 minute exposure.

After each treatment, treated tissue was cut at the center of the image/treatment plane. Ablation histology was evaluated by triphenyl tetrazolium chloride (TTC) vital staining (2% TTC, 45 min). Stained sections were scanned at 1500 dpi using a flatbed scanner (Canonscan 8800F). The scanned images were segmented using ImageJ (National Institutes of Health) as illustrated in Figure 2. The segmented images show three distinct regions based on level of TTC uptake. An inner bleached region shows no TTC uptake due to cessation of enzymatic activity and is considered nonviable or ablated. Surrounding the ablated area is a region staining pink due to reduced metabolic activity resulting in partial TTC uptake. Normal untreated liver takes up TTC completely, causing a dark red appearance, and is considered viable. Areas of tissue ablation (no TTC uptake) and tissue treatment (no or partial TTC uptake) were quantified using ImageJ for the 11 control and 11 overpressure runs.

RESULTS

TTC-stained tissue cross sections for control and overpressure experiments (runs 1 and 2) are shown in Figure 2. Consistent with the overall results given below, the inner ablated area is smaller under overpressure conditions, while the area of partial TTC uptake is larger. The total treated area is comparable.

Time-dependent, dB-scaled power spectra of acoustic emissions for representative control and overpressure experiments (runs 1 and 2) are shown in Figure 3. Consistent with the overall results, these time-frequency surface plots show that the 1.55 MHz subharmonic component decreased in the presence of overpressure. Also consistent

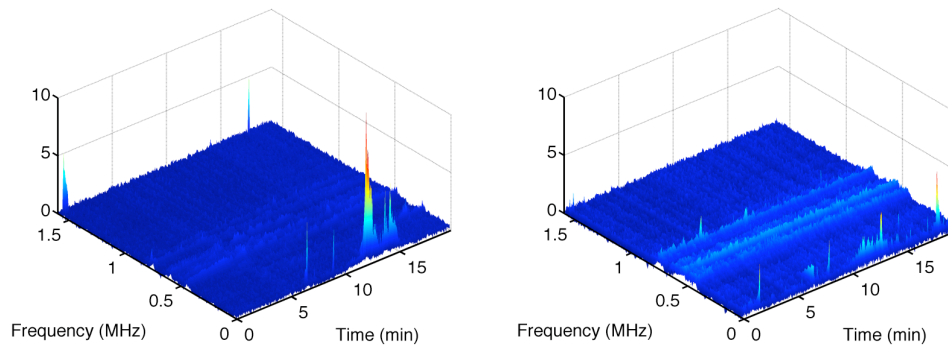


FIGURE 3. Time-dependent power spectra for representative control (left) and overpressure (right) ablation experiments. Each surface plot shows the power spectrum level in dB as a function of time throughout each 20 minute ablation exposure.

with overall results, low-level broadband emissions increased in the presence of overpressure.

Figure 4 summarizes statistics for treatment areas and emission levels for the 11 control and 11 overpressure experiments. Comparison of ablated and treated areas indicates that overpressure reduced the area of ablation in a statistically significant manner (Student t test, $t = -3.03$, $p = 6.65 \cdot 10^{-3}$). Though the overall treated area was slightly smaller under overpressure conditions, this difference was not statistically significant ($t = 1.39$, $p = 0.18$). Overpressure significantly decreased time-average subharmonic emission levels ($t = -2.45$, $p = 2.32 \cdot 10^{-3}$), but significantly increased broadband emission levels ($t = 4.12$, $p = 5.31 \cdot 10^{-4}$), while low-frequency emissions were not significantly altered.

Ablation areas and acoustic emission levels were correlated using regression analysis for each of the control and overpressure experiments. For the control (normal pressure) experiments, the total treated area correlated significantly ($p < 0.05$) with all three defined acoustic emission levels, including subharmonic ($r = 0.630$, $p = 0.0378$), broadband ($r = 0.632$, $p = 0.0369$), and low-frequency emissions ($r = 0.693$, $p = 0.0181$). For the overpressure experiments, the overall treated area was anticorrelated with the time-averaged broadband emission level ($r = -0.608$, $p = 0.0471$). Other correlations between treatment areas and mean acoustic emission levels were not statistically significant ($p > 0.05$).

DISCUSSION

The results reported here suggest that bubble activity significantly influences ultrasound bulk ablation. Application of overpressure suppressed subharmonic emissions associated with stable cavitation, but caused an increase in low-level broadband emissions. This increase in low-level broadband activity is not completely understood, but may be associated with an overpressure-induced change in the size distribution of cavitation nuclei.

Notably, overpressure significantly decreased the area of tissue ablation in these experiments, suggesting that suppression of microbubble activity may decrease heat deposition by bulk ultrasound ablation in liver tissue. This trend is opposite to trends previously observed for HIFU ablation, in which overpressure caused an increase in

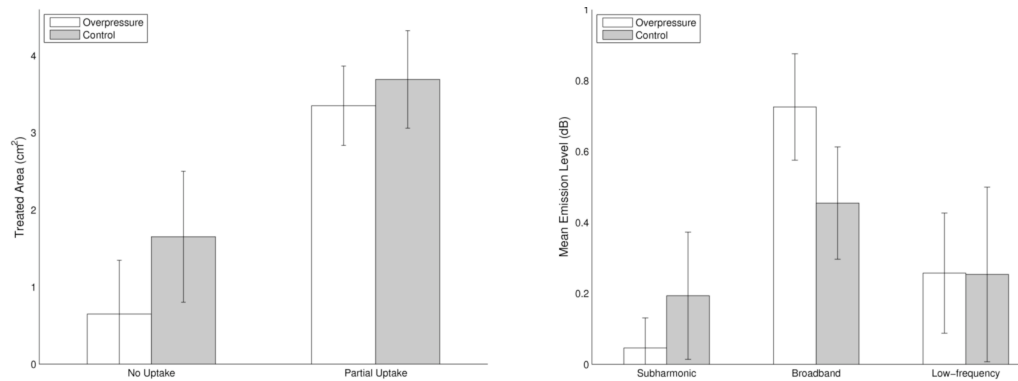


FIGURE 4. Comparison of acoustic emission and ablation results for control and overpressure experiments. Left: comparison of ablated and treated areas. Right: comparison of time-averaged subharmonic, broadband and low frequency emission levels.

thermal lesion size, possibly due to suppression of cavitation-induced focus aberration (Reed 2003). The present study suggests that cavitation plays a different role in bulk ultrasound ablation. For the lower ultrasound intensities employed in ultrasound bulk ablation, the primary effect of cavitation may be an effective increase in tissue absorption due to scattering and microbubble oscillations.

Acknowledgments: This research was supported by a University of Cincinnati Summer Graduate Student Research Fellowship and by NIH grants R43-CA124283 and R01-NS047603. The authors thank Ronald Burrage (Measurement Technologies Inc.) for his help in hand pump construction.

REFERENCES

- Bailey MR, Couret LN, Sapozhnikov OA, Khokhlova VA, ter Haar G, Vaezy S, Shi X, Martin R, Crum LA. Use of overpressure to assess the role of bubbles in focused ultrasound lesion shape *in vitro*. *Ultras Med Biol* 2001; 27:695-708.
- Fry FJ. Intense focused ultrasound in medicine. *Eur Urol* 1993; 23:2-7.
- Makin IRS, Mast TD, Makin IRS, Faidi W, Runk MM, Barthe PG, Slayton MH. Miniaturized ultrasound arrays for interstitial ablation and imaging. *Ultras Med Biol* 2005; 31:1539-1550.
- Mast TD, Makin IRS, Faidi W, Runk MM, Barthe PG, Slayton MH. Bulk ablation of soft tissue with intense ultrasound: modeling and experiments. *J Acoust Soc Am* 2005; 118:2715-2724.
- Mast TD, Salgaonkar VA, Karunakaran CP, Besse JA, Datta S, Holland CK. Acoustic emissions during 3.1 MHz ultrasound bulk ablation *in vitro*. *Ultras Med Biol* 2008; 34:1434-1448.
- Melodelima D, Chapelon JY, Theillère Y, Cathignol D. Combination of thermal and cavitation effects to generate deep lesions with an endocavitary applicator using a plane transducer: *ex vivo* studies. *Ultras Med Biol* 2004; 30, No.1: 103-111.
- National Cancer Institute, <http://www.cancer.gov/cancertopics/types/liver/>, accessed September 2008.
- Rabkin BA, Zderic V, Vaezy S. Hyperecho in ultrasound images of HIFU therapy: involvement of cavitation. *Ultras Med Biol* 2001; 27: 1399-1412.
- Reed JA, Bailey MR, Nakazawa M, Crum LA, Khokhlova LA. Separating nonlinear propagation and cavitation effects in HIFU. *IEEE Ultrasonics Symposium* 2003; 728-731.
- ter Haar GR, Daniels S. Evidence for ultrasonically induced cavitation *in vivo*. *Phys Med Biol* 1981; 26: 1145-1149.
- Watkin NA, ter Haar GR, Rivens I. The intensity dependence of the site of maximal energy deposition in focused ultrasound surgery. *Ultras Med Biol* 1996; 22:483-491.
- Xu Z, Fowlkes JB, Ludomirsky A, Cain AC. Investigation of intensity thresholds for ultrasound tissue erosion. *Ultras Med Biol* 2005; 31: 1673-1682.